OSUN GEOGRAPHICAL REVIEW

Journal of the Department of Geography,
Osun State University, State of Osun, Nigeria

Volume 5, 2022

ISSN: 2695 - 1959

Published by the
Department of Geography, Osun State University,
State of Osun, Nigeria

CONTENTS

OSUN GEOGRAPHICAL REVIEW
Published by the Department of Geography, Osun State University, State of Osun, Nigeria
ISSN: 2695 - 1959 Volume 5, 2022; 21 - 29

IN-SITU SURFACE TEMPERATURE AND THERMAL INFRARED SATELLITE DATA COLLECTION FOR HEAT ISLAND EVALUATION AND DATA COMPARISON IN AN URBAN AREA IN SOUTHWEST NIGERIA

[*1]O.O. Tope-Ajayi, [1]O. H. Adedeji, [1]C. O. Adeofun and [2]A. O. Akingbade

[1]Department of Environmental Management and Toxicology, Federal University of Agriculture, Abeokuta, Nigeria.
[2]African Regional Institute for Geospatial Information Science and Technology, Obafemi Awolowo, Ile Ife, Nigeria.
*Corresponding author: *topeajayiopeyemi@gmail.com*

Abstract

Urban Heat Island (UHI), which is due to differential cooling and heating of land surfaces, can increase the environmental and social vulnerabilities in an urban area. This study validated ground-based surface temperature from the digital infrared thermometer and thermal infrared satellite data to assess heat islands in Ibadan Metropolis, Nigeria. The study employed a single-channel algorithm method (SCA) to retrieve land surface temperature (LST), an important factor in global climate change, vegetation growth, and glacier. This was derived from the thermal band of Landsat-8. The results indicate that the mean surface temperatures derived from Landsat imageries during the study period differ from ground-based measurements in all the sample locations. Satellite-based LST over different locations had a range reading between 26.05 ºC and 29.28 ºC, while ground-based LST over the various communities ranged between 30.04ºC and 32.57ºC. Validation of satellite LST against ground-based LST data for each site yielded an average RMSE of between 3.69 and 5.56. The LSTs estimated for different sites are positively correlated between the two methods, with a correlation coefficient (r) between 0.87 and 0.40. There is a problem with the accuracy of temperature data derived from satellite images, and these problems vary for many reasons.

Keywords: Ground-based measurement**;** Urban heat island; Land surface temperature; Landsat-8; Single-channel algorithm method

Introduction

With rapid urbanisation, the land surface and atmospheric conditions are modified, resulting in higher urban temperatures compared to simultaneous temperatures of the surrounding rural areas, known as the urban heat island (UHI) effect (Quan *et al.,* 2014). The UHI phenomenon indicates the higher air and land surface temperature (LST) in urban areas in comparison to the surrounding rural area primarily caused by increased impervious surface cover replacing evaporative vegetation surfaces and by anthropogenic heat releases (Wengha *et al*., 2004; Rizwan *et al*., 2008; Zhou *et al*., 2017; Zhou *et al.,* 2019). Several researchers have found that natural and socio-economic factors simultaneously affect LST patterns (Kuang *et al*., 2015; Deilami *et al*., 2018; Guha *et al*., 2019).

It is well known and documented that urbanisation leading to UHI can have significant effects on local weather and climate, altering local wind patterns, spurring the development of clouds and fog, increasing the number of lightning events, and influencing the rates of precipitation (Liu and Zhang, 2011; Haas, 2016). UHI produces scorching heat and a range of anomalous urban climates, which significantly affect city-scale climate, industrial activity and the inhabitants' everyday life (Zeng *et al*., 2009).

Urban heat islands have the potential to become one of the most significant problems associated with the urbanisation and industrialisation of human civilisation, as the increased temperatures associated with UHIs tend to exacerbate the threats to human health posed by thermal stress. In fact, the UHI effect and the associated consequences are expected to be more severe under a warming climate and a rapidly urbanising world (Seto *et al.*, 2012; Stocker, 2013; Zhou *et al.*, 2016), particularly in countries like China, India, and Nigeria, which are projected to occupy 35% of the global urban population growth between 2018 and 2050 (UN., 2018; Peng *et al.*, 2018; Zhou *et al.*, 2019).

Geospatial techniques such as GIS and remote sensing have found a wide range of methods of gathering temperature data for urban heat island analysis (Liu and Zhang, 2011; Liao *et al.*, 2017). Thermal data derived from satellite imageries can repeatedly depict the temperature patterns in extensive urban areas because of their spatial coverage and temporal frequency (Rao, 1972; Voogt and Oke, 2003; Deilami *et al.*, 2018). LST has been widely used to reflect UHI variability, especially for local-scale studies based on Landsat series or ASTER data (Song and Wu, 2016; Zhang *et al.*, 2017; Peng *et al.*, 2018), and such studies often concentrate on the LST variations and their relationships with spatial-temporal factors in a city (Yu *et al.*, 2014; Deilami *et al.*, 2018). To prove the validity of satellite temperature measurements, some studies have conducted research by comparing satellite image surface temperature data to temperatures measured onsite. Nichol *et al.* (2005) investigated UHIs. They validated the accuracy of ASTER image surface temperature data by recording surface temperatures at 18 sites located throughout the urban region of Kowloon in Hong Kong and the nonurban area of the New Territories in Hong Kong. Studies of UHI have been conducted in more than 1400 cities worldwide, particularly in China, the US, France and Germany, but very few in cities in Nigeria and many other developing countries (Abegunde and Adedeji, 2015; Odindi *et al.*, 2015; Tarawally *et al.*, 2018). Most of these studies compared low-resolution image temperature data with ground-based temperature measurements. Landsat-8 medium spatial resolution multispectral imagery presents particular interest in extracting land cover (Li and Jiang, 2018) because of the fine spectral resolution and the radiometric quantisation of 12 bits. The specific objectives of this study are to (1) retrieve LST from Landsat 8 OLI and TIRS data and prepare spatial LST distribution maps for Ibadan Metropolis, Nigeria; (2) identify the UHI based on the retrieved LST over the study area and (3) compare and confirm the accuracy of the Landsat 8 OLI and TIRS data and *in situ* temperature readings in the study area.

Materials and Methods

Study area

Ibadan Metropolis is a major urban centre in Nigeria which is located between latitude 7°02' N to 7°40' N and longitude 3°41' E to 4°07' E (Figure 1) with a land mass of 3,114 sqkm and a population of 2,550,593 (Ajayi *et al.,* 2012). It is the capital city of Oyo State, southwestern Nigeria and about 128 km inland northeast of Lagos and 530 km southwest of Abuja (the federal capital).

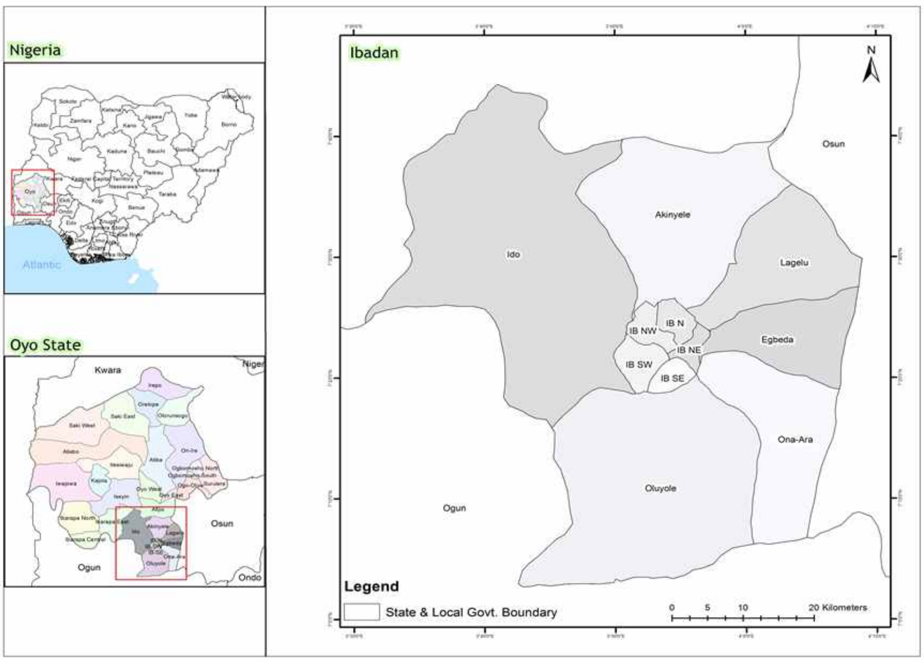

Figure 1: Study area map.

The physical growth of Ibadan is an example of urban expansion in Nigeria, which leads to demand for peripheral land space for development. The city has sprawled into the peripheral areas around the urban centre due to uncontrolled growth, a common feature of the built environment in both the developed and developing countries of the world. Land use/land cover changes caused by the conversion of natural areas to impervious surfaces have decreased evapotranspiration and enhanced absorption and trapping of solar radiation in the urban centres, causing the well-known urban heat island (UHI) phenomenon (Chen *et al.*, 2017). To compute the UHI in this study, seven sites within the urban boundary, including the five local government areas making up the metropolis, were used to collect land surface temperature data. The sites include Alaakia-Ibadan Airport, Ajanle, Beere, Eleyele, University of Ibadan (UI), Oluyole Industrial Estate and Lalupon. These communities were selected because of their diverse land use and coverage characteristics, which varied between urban, densely populated, and suburb, less densely populated, no industrial, and less traffic congestion.

Data collection

For data collection for this study, we considered the LST products from Landsat 8 OLI/TIRS (Operational Land Imager/Thermal Infrared Sensor) and *in-situ* LST temperature with the aid of non-contact digital thermal infrared thermometers. According to the technical specification, the Landsat-8 measurements are very suitable for LST mapping (Li and Jiang, 2018). The widely used single-channel method was adopted to calculate LST from the thermal bands (Thermal bands 10 and 11) of the Landsat image according to the thermal radiant transfer equation (Zhang *et al.*, 2015; Liu and Zhang, 2011; Wang *et al.*, 2019). Landsat 8 and Google Earth data were combined with extensive field checks and surveys (ground-based measurement data) for this analysis. Ground surface temperatures were measured directly using handheld, non-contact digital thermal infrared thermometers, which determine an object's surface temperature by measuring the amount of infrared energy radiated by the object's surface (Song and Park, 2014; Zhang *et al.*, 2015). Table 1 shows the characteristics of the Landsat images used in this research. Among the twelve satellite images downloaded in the year 2020, four with less than 14 % cloud cover were used for analysis.

Satellite images were downloaded, and ground-based observations were obtained based on the following criteria: (1) The images were captured during the study period; (2) Images with more than 14 % cloud cover in the study area were neglected; (3) The ground observation time was within ±1 hour of satellite overpass (Hu and Brunsell, 2014); (4) Non-contact thermal infrared thermometer was held 10 cm vertically and at the closest possible distance off the surface respectively to measure the surface temperature (Song and Park, 2014); (5) The observation sites were within the study domains (Hu and Brunsell, 2014).

Data processing

The study utilised the LST products from Landsat 8 OLI/TIRS (Operational Land Imager/Thermal Infrared Sensor) with a spatial resolution of 100m, which was resampled using the nearest neighbour algorithm with a pixel size of 30 m to match the optical bands. The satellite imageries were geometrically and radiometrically corrected to enhance the image quality.

Satellite image-based surface temperature data were extracted from the thermal infrared (TIR) bands/sensors of Landsat 8. In addition, Google Earth imageries were used to classify the study area into different land use/cover types. This study used four months of Landsat 8 thermal band (January, February, November and December 2020). Ground-based temperature data were obtained at different

Table 1: Characteristics of the Landsat images used

Name	Sensor	Path/ Row	Spatial Resolution(m)	Wavelength (μm)	Acquisition Date
Landsat 8	OLI & TIRS (*Operational Land Imager and Thermal Infrared Sensor*)	191/055	Thermal bands 10 and 11 (100m)	Band 10: 10.60–11.19 (Thermal band) Band 11: 11.50–12.51 (Thermal band)	• 2020/01/20 • 2020/02/21 • 2020/11/03 • 2020/12/21

Source: http://www.landsat.usgs.gov/Landsat8_Using_Product.php parts of the urban and suburbs using a non-contact thermal infrared thermometer for each month at ±1 hour of the satellite overpass. Surface temperatures were extracted with ArcGIS 10.0 software after geometric corrections, and coordinate transformations were performed on the satellite imagery. The mean land surface temperature (LST) for satellite-based data and the ground-based temperature data for the thermal infrared thermometer were compared for the same period for validation. The widely used single-channel algorithm (SCA) method, developed by Jiménez-Muñoz and Sobrino (2003) and later improved by Jiménez-Muñoz *et al*. (2009), was adopted to calculate LST from the thermal band of Landsat data according to the thermal radiant transfer equation (Liu and Zhang, 2011; Jimenez-Munoz *et al*., 2014). The algorithm requires only two input parameters, the Land Surface Emissivity (LSE) (Ɛ) and the atmospheric water vapour content (ω). Accurate determination of the LST using the SCA method also requires a high-quality atmospheric transmittance/radiance code to estimate the atmospheric features involved in the radiative transfer equation (Li *et al*., 2013). Given the larger calibration uncertainty associated with Band 11 (USGS, 2014), the use of a split-window algorithm that relies on Band 11 data is not recommended; therefore, the LST estimated from Band 10 (with weaker absorption) has higher accuracy than Band 11 (Jimenez-Munoz *et al*., 2014; Yu *et al*., 2014). Land Surface Temperature retrieval includes;

1. Converting calibrated digital numbers (DNs) to absolute units of at-sensor spectral radiance;
2. Converting at-sensor spectral radiance to at-sensor brightness temperature (i.e., blackbody temperature), correcting for Land Surface Emissivity,
3. Calculating for kinetic temperature land surface temperature (LST).

Results and Discussion

Field measurements of surface temperatures were used to verify the final retrieved LST results due to the lack of simultaneous land surface temperature data when the satellite passes. Ground-based temperature data were recorded in 2781 locations on different land use/cover types in and around Ibadan in January, February, November and December 2020.

Mean Surface temperatures derived from Landsat imageries during the study period differ from those measured ground-based measurements in all the sample locations. It was observed that the average land surface temperature derived from the satellite data over different communities tends to rise closer to the city centre (Ibadan North, Ibadan North-West, Ibadan North-East, Ibadan South-East and Ibadan South-West). Highly residential areas like Agbadagudu and Beere area had a mean satellite LST reading of 28.6 ºC, while industrial areas, i.e. Oluyole Industrial Estate, had a satellite LST reading of 29.28 ºC. Moving toward the suburbs in areas such as Ajanla, satellite-derived LST gradually reduced to 26.05 ºC because of the scattered nature of the residential buildings and more dense vegetal cover in the area.

The University of Ibadan, an academic institution, has a similar low satellite-derived LST of 26.46 ºC because the area has some preserved natural vegetation (trees), water bodies and agricultural lands. Tumiar and Syarifah (2015) observed a similar situation in Bandar Lampung City, Indonesia, where Tanjung Karang Pusat (city centre), Teluk Betung (business area) and Panjang (coastal area) had high LSTs of between 32–34 ºC compared to Gedung Tataan and Natar (agricultural areas) that had low LSTs of between 27 ºC and 29 ºC. On the other hand, ground-based LSTs were higher than satellite-derived LSTs. The average ground-based LST over the different communities were 32.57 ºC for Oluyole Industrial Estate, followed by Beere, Ibadan Airport and the University of Ibadan with 32.23 ºC, 30.20 ºC, and 30.04 ºC respectively. Suburb areas recorded lower LSTs, with Ajanla and Lalupon recording 29.14 ºC and 29.28 ºC, respectively. Ground-based LST observed in Jakarta, Indonesia, showed a similar high temperature of 35.4 ºC in Johar Baru community (city centre) compared to a lower temperature of 27 ºC in Semanan (farm settlement) (Tumiar and Syarifah, 2015).

There is a noticeable difference in the temperature reading *on-site* using a thermal infrared thermometer and that of satellite in all locations with a varied Root Mean Square Error (RMSE). Validation of at-satellite LST against *in situ* LST data for each site yielded an average RMSE of between 3.69 and 5.56. LSTs estimated for different sites are positively correlated between the two methods of temperature extraction with the correlation coefficient (r) of 0.87, 0.82, 0.82, 0.76, 0.40, 0.76 and 0.80 in Alaakia-Ibadan airport, Ajanta, Beere, Eleyele, Oluyole, Lalupon and the University of Ibadan respectively.

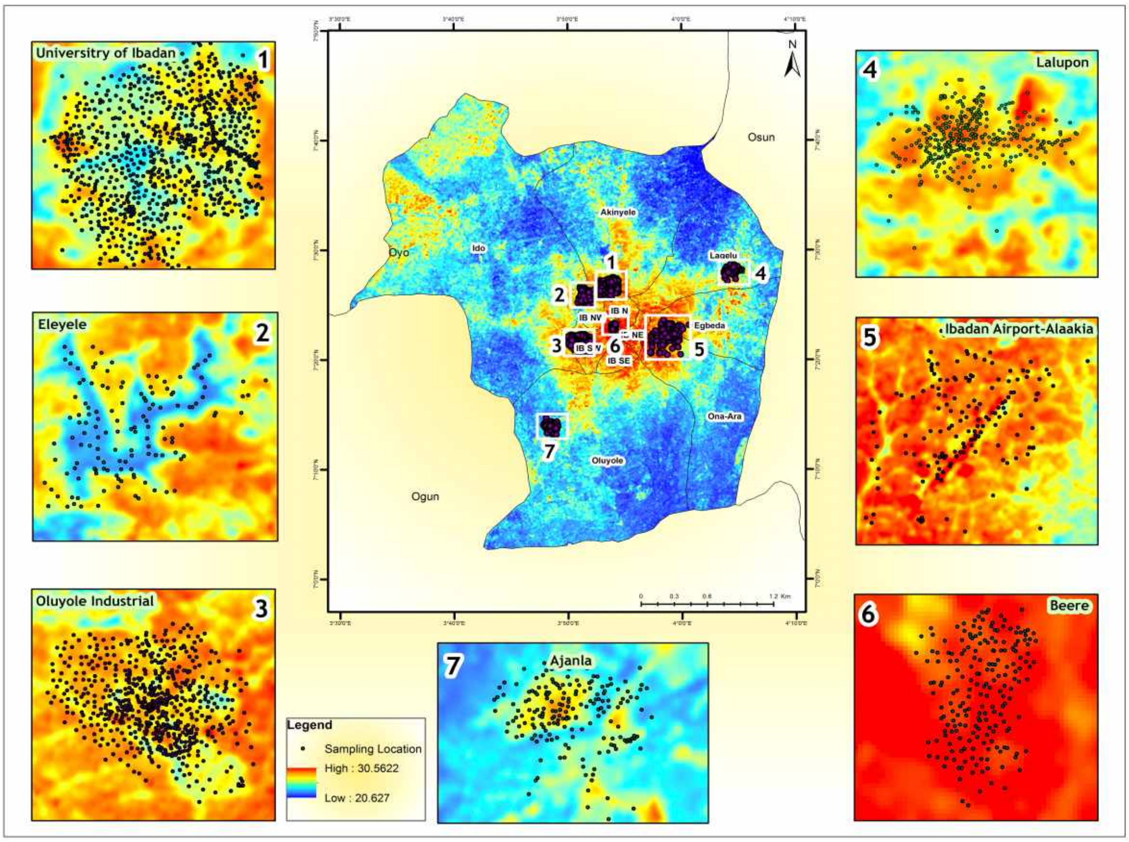

Figure 2: Average Land Surface Temperature (satellite-derived over different communities in Ibadan (2020).

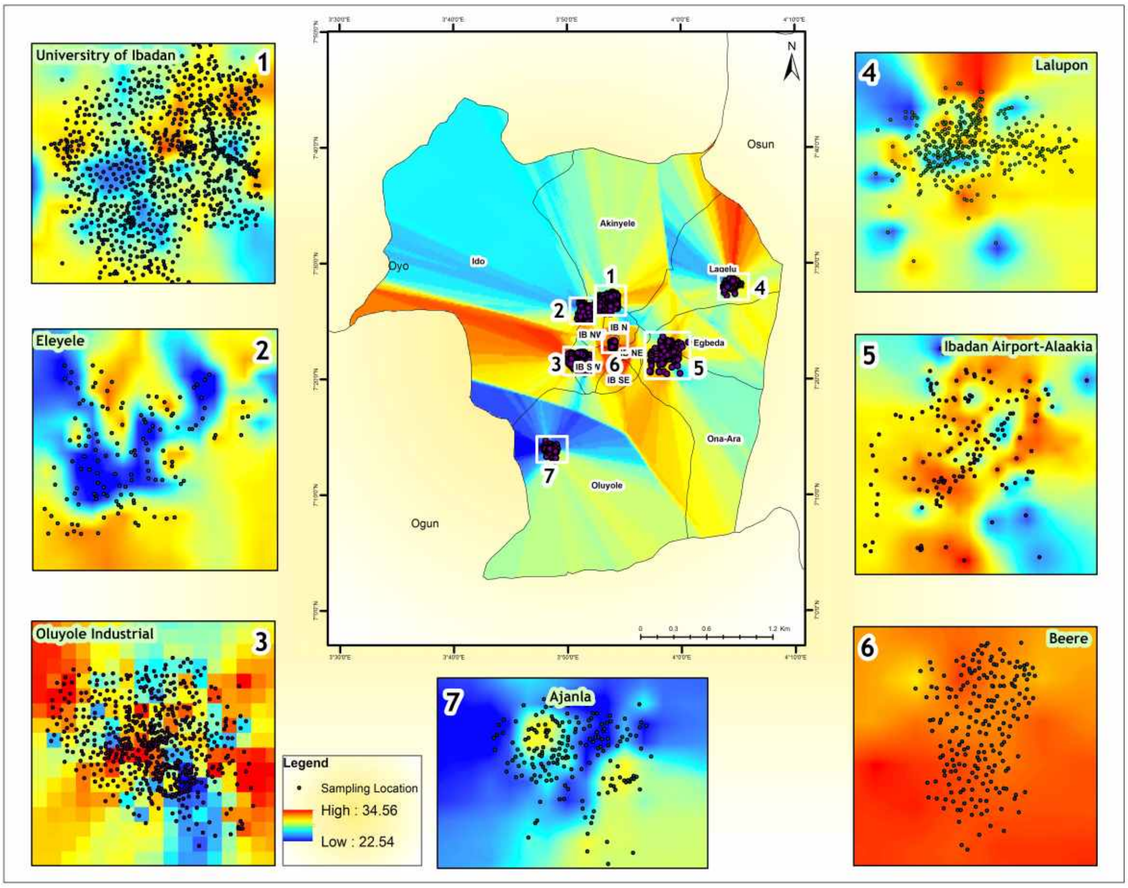

Figure 3: Average Land Surface Temperature (ground-based) over different communities in Ibadan (2020)

From these results, it can be inferred that LST extracted from the thermal band is valid.

Differences between infrared satellite image surface temperature data and onsite temperature measurements at the exact site/location may be caused by population density (Hartz *et al.*, 2006), densely built-up areas (Barring *et al.*, 1985; Eliasson, 1996), off-nadir angle of the satellite image (Song and Park, 2014), limited horizontal surface view of earth's surface (Voogt and Oke, 2003); application of emissivity values that do not consider the complex spatial characteristics of urban (Han *et al.*, 2004) and especially cloud cover (Song and Park, 2014).

The RMSEs obtained in the study were similar to 3.07, 3.18, and 3.02 obtained by Sekertekin and Bonafonim (2020) for radiative transfer equation (RTE), single channel algorithm (SCA) and split window algorithm (SWA), respectively. Furthermore, Zhang *et al.* (2016) also investigated the accuracy of SCA using Landsat 8 imagery and Surface Radiation Budget Network (SURFRAD) measurements using 40 Landsat 8 scenes acquired in different seasons and different years, and they obtained 1.96 RMSE.

Figures 2 and 3 show some UHI hotspots in Ibadan with little or no vegetal covers. Spatial distribution of LST in the study area for January, February, November and December 2020 using ground-based and satellite-derived measurements. The minimum and maximum temperatures were 22.54 °C and 34.56 °C for ground-based and 20.63 °C and 30.58 °C for satellite-derived measurements.

LST distribution was classified into appropriate ranges and colour-coded to generate a thermal pattern distribution map of LST over the study area. A reddish tone highlights higher temperature, while a bluish tone represents lower temperature in LST. The highest temperature distributions were located around the city centre (Ibadan North, Ibadan North-West, Ibadan North-East, Ibadan South-West and Ibadan South-East) in dense high thermal conductors. These areas have high human activities and diverse land use patterns, which create various landuse landcover types, influencing temperature change in and around the study area. According to the distribution maps, LST is usually lower in areas where there is the presence of materials with low thermal conductivity. These areas were found in the suburbs of Ibadan (Akinyele, Ido, Lagelu, Oluyole, Ona-Ara and Egbeda). The effect of land use landcover in the warming or cooling of an area, however, depends on the land use/cover type and the proportion of the total area occupied by each type.

The trend of LST in this study is similar to that of an earlier study in Ibadan, which showed that the lowest temperature was located towards the western part of Ibadan, corresponding to densely vegetated areas and consisting of the waterbody (Abegunde and Adedeji, 2015). LST change is correlated spatially with LULC (Zhang *et al.*, 2016; Deilami and Kamruzzaman, 2017). LST also correlates differently with LULC indices for a whole city or a small UHI zone formed within the city boundary (Guha *et al.*, 2019).

In the city centre, buildings reduce heat removal by advection and reduce the sky view factor, thus limiting heat escape to space, while walls and pavements absorb and emit heat (Adebowale and Kayode, 2015; Ning *et al.*, 2017; Tarawally *et al.*, 2018) causing large amounts of stagnant heat and high temperatures, especially in closely packed and high rise buildings. The results also clearly show that LST is sensitive to changes in vegetation density and captures additional information on the biophysical controls on surface temperature, such as surface roughness and transpirational cooling. The relationship between landscape pattern and UHI has become globally considerable (Chen *et al.*, 2014; Peng *et al.*, 2016), and several studies have shown that elevated temperature results in increased outdoor and indoor human thermal discomfort, as well as increased heat-related health risk (Harlan *et al.*, 2013; Gronlund *et al.*, 2015).

The ground-based measurements used in this study ensured the correctness of the results obtained from the satellite-derived data. It is one of the three standard methods for verifying the results of LST. The method adopted is simple and accurate because it compares the retrieved LST with the LST measured in the field, and the accuracy of the retrieved LST can be verified (Yang *et al.*, 2017). The most critical problem in LST validation might be the accuracy and representativeness of the ground-truth LST at the satellite pixel scale (Li *et al.*, 2013). The study's results confirmed the accuracy of the ground-based and satellite-derived LST measurements using Landsat 8 imagery. The difference between the two methods of estimating LST values can be associated partly with the effects of surface roughness on surface temperature and emissivity not considered (Weng, 2009) and partly because of atmospheric impurities obstructing the smooth passage of radiant energy (Ngie, 2020). In addition, the spatio-temporal comparison among LST retrieval methods revealed that they have a high level of agreement with each other regardless of the time. The two methods showed good results for the LST retrieval method, with the highest RMSE being 5.56 in Oluyole Industrial Estate. Ground-based validation is considered to be the most reliable validation technique; however, measurements of the ground-truth LST are limited by the difficulty of finding a homogeneous region as large as the satellite pixel size and by the difficulty and associated costs of sampling over heterogeneous landscapes (Li *et al.*, 2013). Therefore, LST retrieval methods using satellite data are generally recommended because the accuracy of the radiometric measurements and emissivity is the primary uncertainty for ground-based LST retrievals (Sobrino and Skoković, 2016; Guillevic *et al.*, 2018).

Conclusion

This study compared LST retrieved from medium spatial resolution multispectral imagery, i.e. Landsat-8 TIRS Band 10, using the improved single-channel algorithm (SCA) method and ground-based temperature data to measure UHI in Ibadan Metropolis, Nigeria. This study confirmed problems with the accuracy of surface temperature data derived from satellite images, which vary according to the time, place and the presence of different urban characteristics. Often, areas of high density displayed more significant temperature irregularities than vegetated areas. The difference in temperature between ground-based and satellite-based measurements was also affected by whether the surface fabric was artificial or not.

During this study period, communities around the city centre or in the city experienced higher temperatures related to the presence and activities of humans. Places like Oluyole Industrial, Beere-Agbadagudu, and Alakia-Ibadan airport, experienced higher ambient temperatures throughout the study period and the Ajanla area and Lalupon are cooler. The presence of natural land cover in the suburbs of Ibadan can be traced to its natural cooling effect. The wide range of RMSE between ground-based and satellite measurements was due to significant factors mentioned earlier in the study. Regression analysis was explored to decide the relationship between the two land surface temperature measurements in which ground-based LSTs were positively correlated with the calculated satellite-based measurement.

UHI actually exist in Ibadan based on this research finding, and its effect may be related to land use/cover patterns. A non-complex and revised method or model of acquiring temperature data from Landsat Imagery and emissivity values from different land covers are proposed to improve the correctness of surface temperatures extracted from Landsat satellite imagery. GIS, remote sensing and statistical models have been helpful to a considerable extent in assessing and validating data and methods that we use in day-to-day studies to check and prevent discrepancies.

Although LST retrieval is still challenging, there is a need to conduct more research to improve the accuracy of satellite-derived LST because it is a fundamental aspect of climate and biology, which affect organisms and ecosystems from local to global scales.

References

Abegunde, L. and Adedeji, O. (2015). Impact of Landuse Change on Surface Temperature in Ibadan, Nigeria. *International Journal of Environmental and Ecological Engineering,* 9(3), 235-240

Adebowale, B.I. and Kayode, S.E. (2015). Geospatial Assessment of Urban Expansion and Land Surface Temperature in Akure, Nigeria. In *Proceedings of the ICUC9—9th International Conference on Urban Climate Jointly with 12th Symposium on the Urban Environment, Toulouse, France*, 20–24 July 2015; pp. 1–6.

Chen, A., Yao, X.A., Sun, R., and Chen, L. (2014). Effect of urban green patterns on surface urban cool islands and its seasonal variations. *Urban Forestry & Urban Greening*, 13, 646–654.

Chen,W.; Zhang, Y.; Pengwang, C.; Gao,W. (2017). Evaluation of Urbanization Dynamics and Its Impacts on Surface Heat Islands: A Case Study of Beijing, *China. Remote Sens.* 9, 453.

Deilami, K.; Kamruzzaman, M.; Liu, Y. (2018). Urban heat island effect: A systematic review of spatio-temporal factors, data, methods, and mitigation measures. *Int. J. Appl. Earth Obs. Geoinf.* 67, 30–42.

Deilami, K., and Kamruzzaman, M. (2017). Modelling the urban heat island effect of smart growth policy scenarios in Brisbane. *Land Use Policy*, 64, 38–55.

Gronlund, C.J., Berrocal, V.J., White-Newsome, J.L., Conlon, K.C., O'Neill, M.S. (2015). Vulnerability to extreme heat by socio-demographic characteristics and area green space among the elderly in Michigan, 1990–2007. *Environ. Res.*, 136, 449–461.

Guha, S., Govil, H., Dey, A. and Gill, N. (2019). Analytical study of land surface temperature with NDVI and NDBI using Landsat 8 OLI and TIRS data in Florence and Naples city, Italy, *European Journal of Remote Sensing,* 51:1, 667-678.

Guillevic, P., Göttsche, F., Nickeson, J., Hulley, G., Ghent, D., Yu, Y., Trigo, I., Hook, S., Sobrino, J.A., Remedios, J. (2018). Land Surface Temperature Product Validation Best Practice Protocol; In Guillevic, P., Göttsche, F., Nickeson, J., Román, M., (Eds.); *Version 1.1; CEOS WGCV* Land Product Validation Subgroup: Greenbelt, MD, USA, 2018.

Harlan, S. L., Declet-Barreto, J. H., Stefanov, W. L., Petitti, D. B. (2013). Neighborhood effects on heat deaths: Social and environmental predictors of vulnerability in Maricopa county, Arizona. *Environ. Health Perspect.* 121, 197–204.

Huang, B., Wang, J., Song, H., Fu, D., Wong, K. (2013). Generating high spatiotemporal resolution land surface temperature for urban heat island monitoring. *IEEE Geosci. Remote Sens. Lett.*, 10, 1011–1015.

Jiménez-Muñoz, J. C., Sobrino, J. A. (2003). A generalized single-channel method for retrieving land surface temperature from remote sensing data. *J. Geophys. Res. Atmos.*, 108.

Jiménez-Muñoz, J.C.; Cristóbal, J.; Sobrino, J.A.; Sòria, G.; Ninyerola, M.; Pons, X. 2009, Revision of the Single-Channel Algorithm for Land Surface Temperature Retrieval From Landsat Thermal-Infrared Data. *IEEE Trans. Geosci. Remote Sens.,* 47, 339–349.

Jimenez-Munoz, J. C., Sobrino, J. A., Skokovic, D., Mattar, C., Cristobal, J. (2014). Land surface temperature retrieval methods from Landsat-8 thermal infrared sensor data. *IEEE Geosci. Remote Sens. Lett.*, 11, 1840–1843

Li, S. and Jiang, G.M. (2018). Land Surface Temperature Retrieval from Landsat-8 Data with the Generalized Split-Window Algorithm, *IEEE Access. 6,* 18149-18162. *Doi: 10.1109/ACCESS.2018.2818741*

Li, Z. L., Tang, B. H., Wu, H., Ren, H., Yan, G., Wan, Z., Trigo, I.F. and Sobrino, J. A. (2013). Satellite-derived land surface temperature: Current status and perspectives. *Remote Sens. Environ.*, *131*, 14–37.

Liao, W. L., Liu, X. P., Wang, D. G., Sheng, Y. L. (2017). The impact of energy consumption on the surface urban heat island in China's 32 major cities. *Remote Sens*. 9, 250.

Mirzaei, P. A., Haghighat, F. (2010). Approaches to study urban heat island—Abilities and limitations. *Build. Environ*. 45, 2192–2201.

Mohamed, A.A., Odindi, J., Mutanga, O. (2017). Land surface temperature and emissivity estimation for urban heat island assessment using medium- and low-resolution space-borne sensors: A review. *Geocarto Int*. 32, 455–470.

Munoz, J.C., Cristóba, J., Sobrino, J.A., Soria, G., Ninyerola, M., & Pons, X. (2009). Revision of the single-channel algorithm for land surface temperature retrieval from Landsat thermal-infrared data. *Photogrammetric Engineering & Remote Sensing*, 47(1), 339–349.

Ngie, A. (2020). Thermal Remote Sensing of Urban Climates in South Africa through the Mono-Window Algorithm. *The International Archives of the Photogrammetry, Remote Sensing and Spatial Information Sciences, Volume XLII-3/W11, 2020 PECORA 21/ISRSE 38 Joint Meeting, 6–11 October 2019,* Baltimore, Maryland, USA pp.117-123

Ning, J., Gao, Z., Meng, R., Xu, F. and Gao, M. (2017). Analysis of relationships between land surface temperature and land use changes in the Yellow River Delta. *Front. Earth Sci*.

Nichol, J. (2005). Remote sensing of urban heat islands by day and night. *Photogramm. Eng. Remote Sens.* 71, 613–621.

Odindi, J. O., Bangamwabo, V., Mutanga, O., (2015). Assessing the value of urban green spaces in mitigating multi-seasonal urban heat using MODIS Land Surface Temperature (LST) and Landsat 8 data. *Int. J. Environ. Res*. 9, 9–18.

Oke, T. R. (1982). The energetic basis of the urban heat island. *Q. J. R. Meteorol. Soc.* 1982, 108, 1–24.

Peng, J., Xie, P., Liu, Y., and Ma, J., (2016). Urban thermal environment dynamics and associated landscape pattern factors: A case study in the Beijing metropolitan region. *Remote Sensing of Environment,* 173, 145–155.

Peng, J., Ma, J., Liu, Q., Liu, Y., Hu, Y., Li, Y., Yue, Y. (2018). Spatial-temporal change of land surface temperature across 285 cities in China: An urban-rural contrast perspective. *Sci. Total Environ*. 35, 487–497.

Qin, Z., Karnieli, A., and Berliner, P., (2001). A mono-window algorithm for retrieving land surface temperature from Landsat TM data and its application to the Israel–Egypt border region. *International Journal of Remote Sensing*, 22(18), 3719–3746.

Rao, P. K. (1972). Remote sensing of urban "heat islands" from an environmental satellite. *Bull. Am. Meteorol. Soc.*, 53, 647–648.

Rizwan, A. M., Dennis, L. Y. C., Liu, C. (2008). A review on the generation, determination and mitigation of urban heat islands. *J. Environ. Sci.,* 20, 120–128

Sekertekin, A and Bonafoni, S. (2020). Land Surface Temperature Retrieval from Landsat 5, 7, and 8 over Rural Areas: Assessment of Different Retrieval

Algorithms and Emissivity Models and Toolbox Implementation. *Remote Sens.* 2020, 12, 294; doi:10.3390/rs12020294.

Seto, K. C., Güneralp, B., Hutyra, L.R. (2012). Global forecasts of urban expansion to 2030 and direct impacts on biodiversity and carbon pools. *Proc. Natl. Acad. Sci. USA,* 109, 16083–16088.

Sobrino, J. A., Oltra-Carrió, R. and Jiménez-Muñoz J. C. (2012). Emissivity mapping over urban areas using a classification-based approach: application to the Dual-use European Security IR Experiment (DESIREX), *International Journal of Applied Earth Observation and Geoinformation*, 18, 141–147.

Sobrino, J., and Skoković, D. (2016). Permanent stations for calibration/validation of thermal sensors over Spain. *Data,* 1, 10.

Sobrino, J.A., Jiménez-Muñoz, J. C. El-Kharraz, J., Gómez, M., Romaguera, M. and Sòria, G. (2004). Single-channel and two-channel methods for land surface temperature retrieval from DAIS data and its application to the Barrax site. *International Journal of Remote Sensing*, 25, 215-230. https://doi.org/10.1080/ 0143116031000115210

Song, B. and Park, K., (2014). Validation of ASTER Surface Temperature Data with In Situ Measurements to Evaluate Heat Islands in Complex Urban Areas. *Advances in Meteorology, Volume 14, pp 1-12.*

Song, Y.Wu, C. E. (2016). Examining the impact of urban biophysical composition and neighbouring environment on surface urban heat island effect. *Adv. Space Res.* 57, 96–109.

Stocker, T. (2013). *Climate Change: The Physical Science Basis*: Working Group I Contribution to the Fifth Assessment Report of the Intergovernmental Panel on Climate Change; Cambridge University Press: Cambridge, UK.

Tarawally, M., Xu, W., Hou, W. and Mushore, T.D. (2018). Comparative Analysis of Responses of Land Surface Temperature to Long-Term Land Use/Cover Changes between a Coastal and Inland City: A Case of Freetown and Bo Town in Sierra Leone. *Remote Sens*., 10(1), 112; https://doi.org/10.3390/rs10010112.

UN. (2018). United Nations Department of Economic Social Affairs Population Division. *World Urbanization Prospects: The 2018 Revision*; Online Edition; United Nations: New York, NY, USA.

Voogt, J. A. and Oke, T. R. (2003). Thermal remote sensing of urban climates. *Remote Sensing of Environment 86,* 370-84.

Wang, K., Jiang, S., Wang, J., Zhou, C., Wang, X., Lee, X., (2017). Comparing the diurnal and seasonal variabilities of atmospheric and surface urban heat islands based on the Beijing urban meteorological network. *J. Geophys. Res. Atmos*, 122, 2131–2154.

Wang, L., Liu, Y. and Yao, Y. (2019). Comparison of Three Algorithms for the Retrieval of Land Surface Temperature from Landsat 8 Images. *Sensors*, 19, 5049; doi:10.3390/s19225049.

Weng, Q. (2009). Thermal infrared remote sensing for urban climate and environmental studies: Methods, applications, and trends. *ISPRS J. Photogramm. Remote Sens.* 64, 335–344.

Yang, C., He, X., Wang, R., Yan, F., Yu, L., Bu, K., Yang, J., Chang, L. and Zhang, S. (2017). The Effect of Urban Green Spaces on the Urban Thermal Environment and Its Seasonal Variations. *Forests*, 8, 153.

Yu, X., Guo, X. and Wu, Z. (2014). Land Surface Temperature Retrieval from Landsat 8 TIRS—Comparison between Radiative Transfer Equation-Based Method, Split Window Algorithm and Single Channel Method. *Remote Sens. 6*, 9829-9852; doi:10.3390/rs6109829.

Zhang, L., Meng, Q., Sun, Z. and Sun, Y., (2017). Spatial and temporal analysis of the mitigating effects of industrial relocation on the surface urban heat island over China. *ISPRS Int. J. Geoinf.* 6, 121.

Zhang, Z., He, G., Wang, M., Long, T., Wang, G., and Zhang, X. (2016). Validation of the generalized single-channel algorithm using Landsat 8 imagery and SURFRAD ground measurements. *Remote Sens. Lett,* 7, 810–816.

Zhang, X., Pang, J. and Li, L. (2015). Estimation of Land Surface Temperature under Cloudy Skies Using Combined Diurnal Solar Radiation and Surface Temperature Evolution. *Journal of Remote Sensing. v 7, pp 905-921.*

Zhou, B., Rybski, D., Kropp, J. P. (2017). The role of city size and urban form in the surface urban heat island. Sci. Rep., 7, 4791.

Zhou, D., Zhao, S., Zhang, L., Liu, S. (2016). Remotely sensed assessment of urbanization effects on vegetation phenology in China's 32 major cities. *Remote Sens. Environ.* 176, 272–281.

Zhou, D., Xiao, J., Bonafoni, S., Berger, C., Deilami, K., Zhou, Y., Frolking, S., Yao, R., Qiao, Z. and Sobrino, J. A. (2019). Satellite Remote Sensing of Surface Urban Heat Islands: Progress, Challenges, and Perspectives. *Remote Sens,* 11, 48; doi:10.3390/rs1101004.

On line Source

http://www.landsat.usgs.gov/Landsat8_Using_Product.php